Original article

Sensitive detection of alkaline phosphatase based on terminal deoxynucleotidyl transferase and endonuclease IV-assisted exponential signal amplification

Weicong Ye [a,1], Longjie Li [a,b,1], Zishan Feng [a], Bocheng Tu [a], Zhe Hu [a], Xianjin Xiao [c], Tongbo Wu [a,*]

[a] Department of Pharmaceutical Analysis, School of Pharmacy, Tongji Medical College, Huazhong University of Science and Technology, Wuhan, 430030, China
[b] Department of Biopharmaceutics, School of Life Science and Technology, Wuhan Polytechnic University, Wuhan, 430023, China
[c] Department of Translational Medicine, Institute of Reproductive Health, Tongji Medical College, Huazhong University of Science and Technology, Wuhan, 430030, China

ARTICLE INFO

ABSTRACT

Alkaline phosphatase (ALP) is widely expressed in human tissues. ALP plays an important role in the dephosphorylation of proteins and nucleic acids. Therefore, quantitative analysis of ALP plays a vital role in disease diagnosis and the development of biological detection methods. Terminal deoxynucleotidyl transferase (TdT) catalyzes continuous polymerization of deoxynucleotide triphosphates at the 3′-OH end of single-stranded DNA in the absence of a template. In this study, we developed a highly sensitive and selective method based on TdT and endonuclease IV (Endo IV) to quantify ALP activity. After ALP hydrolyzes the 3′-PO$_4$ end of the substrate and generates 3′-OH, TdT can effectively elongate the 3′-OH end with deoxynucleotide adenine triphosphate (dATP) and produce a poly A tail, which can be detected by the poly T probes. Endo IV digests the AP site in poly T probes to generate a fluorescent signal and a new 3′-OH end, leading to the generation of exponential fluorescence signal amplification. The substrate for TdT elongation was optimized, and a limit of detection of 4.3×10^{-3} U/L was achieved for ALP by the optimized substrate structure. This method can also detect ALP in the cell lysate of a single cell. This work has potential applications in disease diagnosis and biomedical detection.

© 2021 The Authors. Published by Elsevier B.V. on behalf of Xi'an Jiaotong University. This is an open access article under the CC BY-NC-ND license (http://creativecommons.org/licenses/by-nc-nd/4.0/).

1. Introduction

Alkaline phosphatase (ALP) is widely present in the human intestine, liver, kidneys, bone, and other tissues. ALP plays an important role in the dephosphorylation of proteins and nucleic acids [1]. As a valuable biomarker for pathological diagnosis, ALP activity is often used as an indicator for diagnosing liver dysfunction, diabetes, and other diseases [2,3]. In environmental biology, monitoring ALP activity can help control phytoplankton population [4–6]. ALP is also used as a signal generation tool in commonly used biological detection methods, such as immunohistochemistry staining and enzyme-linked immunosorbent assay (ELISA). When the ALP-labeled antibody binds to the antigen, ALP can catalyze the chromogenic reaction to reveal antigen-antibody binding [7,8]. Applications in the above fields require accurate quantitative analysis of ALP. Thus, it is imperative to develop a simple, sensitive, and rapid method to detect ALP activity.

The analytical methods for detecting ALP activity include fluorescence analysis, electrochemical biosensors, colorimetry, and chromatography [9–13]. Among them, fluorescence analysis offers the advantages of high sensitivity, low cost, and easy operation. Fluorescence-based methods for ALP detection can be divided into two strategies. The first is based on the direct method, in which the ALP activity is directly reflected by the fluorescence difference between the initial phosphorylated substrate and the dephosphorylated substrate produced by ALP [14–17]. However, the limit of detection (LOD) is not satisfactory in such methods. The second strategy is indirect methods based on dephosphorylated products to trigger subsequent reactions with fluorophore-labeled materials

such as nanomaterials or DNA probes [18−21]. Under this strategy, the reactant can trigger a change in the label to realize ALP activity analysis. This strategy is more stable and highly sensitive for generating fluorescence signals than the first strategy. However, the preparation of nanomaterials is complicated, which limits their widespread applications. For DNA probe-based methods, signal amplification is not easy to design, and time-consuming steps are involved to achieve high sensitivity. Thus, building fluorescence analytical methods compatible with high sensitivity and simple design remains a challenge.

Terminal deoxynucleotidyl transferase (TdT) catalyzes the continuous polymerization of deoxynucleotide triphosphates (dNTPs) at the 3′-OH end of the single-stranded DNA in the absence of a template [22]. Owing to its unique catalytic performance, TdT is often used as a tool enzyme for DNA nanostructure assembly and biological detection [23−25]. As the reaction efficiency of TdT to the 3′-PO$_4$ end is relatively lower than that of the 3′-OH end, TdT could be used to detect ALP with the second strategy mentioned above. For example, TdT-mediated hemin/G-quadruplex DNAzyme nanowires were used to develop an electrochemical assay to detect ALP activity, with an LOD of 0.03 U/L [26]. Furthermore, the TdT-mediated thymine-Hg^{2+}-thymine structure was also used to determine ALP activity, with an LOD of 0.025 U/L [27]. However, these methods require complicated reactants or toxic heavy metals. In this study, we developed a novel exponential amplification detection system based on TdT and endonuclease IV (Endo IV) for detecting ALP activity with higher sensitivity.

As shown in Scheme 1, the phosphate group at the 3′ end of the substrate can serve as the recognition site for ALP. When ALP hydrolyzes 3′-PO$_4$ and generates 3′-OH, TdT can effectively elongate the 3′-OH end with deoxynucleotide adenine triphosphate (dATP) in the solution and produce a poly A tail. The poly A tail serves as the "landing platform" for poly T probes through T:A base pair hybridization. The poly T/poly A double-stranded DNA (dsDNA) is a preferred substrate for Endo IV, which cleaves the AP site in the middle of the poly T probe. As a result, the poly T probe breaks and dissociates from the poly A tail. The fluorophore (FAM) and the black hole quencher-1 (BHQ-1) labeled on two sides of the AP site in the probe separate from each other. Therefore, the fluorescence signal of FAM, which was initially quenched by BHQ-1, is released. As the hydrolysis of the AP site also generates a 3′-OH end, a new poly A tail can be elongated by TdT. Thus, one ALP generates

multiple poly A tails after one TdT and Endo IV catalysis cycle. As the above process is repeated, exponential fluorescence signal amplification can be achieved. Compared to the previous TdT-based methods for ALP detection, our detection system offers the following advantages: use of fewer primary reactants as only two tool enzymes are used; a simpler preparation process, without involving organic compounds or having difficulty in synthesizing quantum dots; and reduced environmental pollution since no toxic heavy metals such as mercury ions are used.

2. Materials and methods

2.1. Materials and reagents

All oligonucleotides used in this study were synthesized and purified by Sangon Biotech Co., Ltd. (Shanghai, China). ALP, TdT, bovine serum albumin (BSA), exonuclease III (Exo III), T7 exonuclease (T7 exo), deoxyribonuclease I (DNase I), uracil glycosylase (UDG), CutSmart reaction buffer (50 mM KAc, 20 mM Tris-Ac, 10 mM Mg(Ac)$_2$, 100 μg/mL BSA, pH 7.9, 25 °C), 10 × TdT buffer (500 mM KAc, 200 mM Tris-Ac, 100 mM Mg(Ac)$_2$, pH 7.9), and 2.5 mM CoCl$_2$ solution were purchased from New England Biolabs Inc. (Ipswich, MA, USA). dATP, agarose, loading buffer, DNA ladder mix, and nucleic acid dye GelRed were purchased from Sangon Biotech Co., Ltd. (Shanghai, China). The concentration of DNA oligonucleotides was measured using a NanoDrop 2000 UV−vis spectrophotometer (Thermo Fisher Scientific, Waltham, MA, USA). The sequences of all oligonucleotides are listed in Table S1.

2.2. Fluorescence monitoring

Fluorescence was measured using a LineGene Mini FQD-16A (Bioer Technology Co., Ltd., Hangzhou, China) at 37 °C. The fluorescence intensity was recorded every 20 s for 120 min, and the gain level was 8. The excitation and emission wavelengths were set to 485 and 582 nm, respectively.

2.3. Feasibility verification and substrate optimization

The reaction system consisting of 200 nM (final concentration for all reagents below) probe, 100 nM substrate, 100 U/mL TdT, 1 × TdT buffer, and 1 mM dATP was incubated at 37 °C for 30 min.
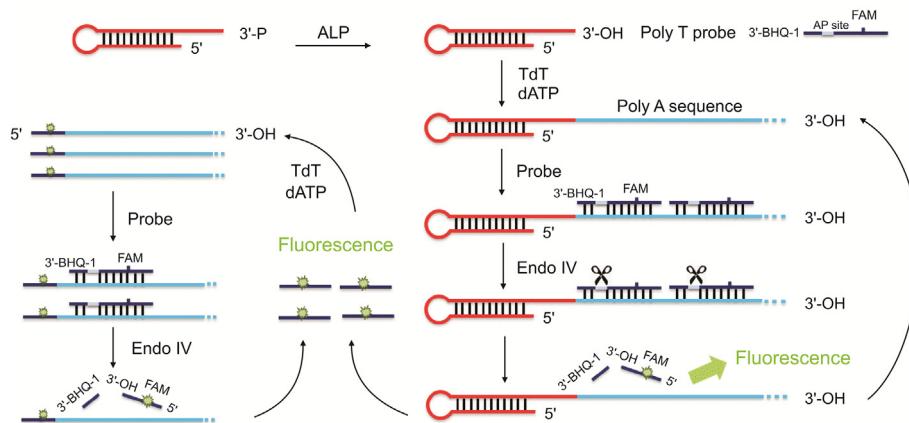
Scheme 1. A schematic illustration of TdT/Endo IV-assisted exponential amplification for ALP detection. ALP: alkaline phosphatase; TdT: terminal deoxynucleotidyl transferase; dATP: deoxynucleotide adenine triphosphate; Endo IV: endonuclease IV; FAM: fluorophore; BHQ-1: black hole quencher-1.

Subsequently, Endo IV (4 U/mL) was added, and the fluorescence intensity was recorded immediately.

2.4. Assay of ALP activity

The reaction system consisting of 200 nM probe, 100 nM L008, $1 \times$ CutSmart reaction buffer, and ALP at various concentrations (0, 0.01, 0.05, 0.1, 0.14, 0.2, 0.3, and 0.4 U/L) was incubated at 37 °C for 30 min. Then, 100 U/mL TdT, $1 \times$ TdT buffer, 1 mM dATP, and the above solutions were incubated at 37 °C for 30 min. Finally, Endo IV (4 U/mL) was added, and the fluorescence intensity was recorded immediately.

2.5. Selectivity of the method

Four enzymes (10 U/L T7 exo, 10 U/L DNase I, 10 U/L UDG, and 10 U/L Exo III) were chosen as the potential interfering enzymes, and 0.1 mg/mL BSA was selected as the interfering non-related protein with 1 U/L ALP in the same reaction. Fluorescence detection was performed under the conditions described above.

2.6. ALP activity detection in biological samples

Approximately 10^6 HeLa cells were pelleted by centrifugation (3000 rpm, 5 min, 4 °C) and resuspended in 90 μL lysis buffer (50 mM Tris-HCl, 150 mM NaCl, 1% NP-40, 0.1% SDS, pH 7.4) on ice. To remove insoluble substances such as DNA, the mixture solution was centrifuged at 12,000 r/min for 30 min at 4 °C. ALP activity was detected in biological samples using the ALP activity assay except that ALP was replaced by cell lysates prepared with different numbers of cells (with 0, 1, 2, 4, 10, 25, and 50 cells).

3. Results and discussion

3.1. Feasibility of the strategy for ALP detection

We first compared the fluorescence signals in the following groups: 1) probe only; 2) probe and poly A strand; 3) probe and 3′-OH strand (simulating the substrate after complete dephosphorylation by ALP); 4) probe, substrate, and ALP; and 5) probe, substrate
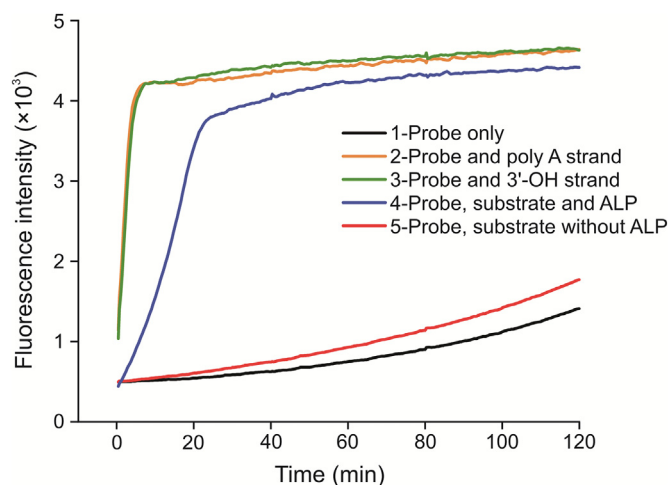

Fig. 1. Fluorescence responses of TdT/Endo IV-assisted amplification under different conditions. The poly A strand is 011-strand-poly A. The substrate is L007-strand-+6ntT. The phosphorylated strand is 007-strand-+6ntT. The sequences of the probe and other strands are shown in Table S1. The y-coordinate reflects the relative fluorescent intensity for the instrument LineGene Mini FQD-16A with a gain level of 8. ALP: alkaline phosphatase.

without ALP. As illustrated in Fig. 1, the fluorescence signal increased very rapidly for groups 2 (orange line) and 3 (green line), indicating that the TdT/Endo IV-assisted signal amplification system worked well for the 3′-OH substrate. A significant fluorescence increase was observed in group 4 (blue line), but the fluorescence increase for group 5 (red line) was slight and similar to that of group 1 (black line). These results demonstrated the feasibility of the design for detecting ALP activity.

Agarose gel electrophoresis was performed to demonstrate the proposed working mechanism. As shown in Fig. S1A, the band in lane 3 was more delayed than that in lane 2, proving that TdT could effectively elongate the substrate with 3′-OH (lane 3) rather than with 3′-PO₄ (lane 2). When ALP was added, 3′-PO₄ was converted into 3′-OH, and TdT elongated the substrate to form a lagged band in lane 4. With further addition of Endo IV and the probe, the green fluorescence emitted by the hydrolyzed probe could be seen under UV light (Fig. S1B, lanes 5 and 6). This further verified that the poly A tail and the probe could form dsDNA after TdT worked, and Endo IV could digest the probe in dsDNA. Furthermore, lane 5 showed a lower migration rate to lane 6 because TdT in lane 6 was inactivated after 30 min of incubation at 37 °C before Endo IV and the probe were added. Thus, in lane 6, the 3′-OH produced by Endo IV by cutting the probe could not be elongated by TdT. Thus, the band in lane 6 is similar to that in lane 4. The entire procedure in Scheme 1 is realized in lane 5. TdT could use the 3′-OH produced by Endo IV to produce a larger poly A structure.

We also performed corresponding fluorescence experiments for lanes 5 and 6 in the gel electrophoresis experiment to confirm the exponential amplification characteristics of our method. As shown in Fig. S2, for the experimental conditions in lane 5 (active TdT), the fluorescence curve exhibited S-type exponential amplification (black line). For the experimental conditions in lane 6 (inactive TdT), the fluorescent signal increased linearly (red line). These results indicated the successful implementation of dual enzymatic-assisted exponential amplification and the feasibility of the design for ALP activity detection.

3.2. Optimization of the TdT/Endo IV-assisted exponential amplification

To increase the sensitivity of the system, we evaluated and optimized the influencing factors of the system. It has been reported that TdT prefers single-stranded DNA (ssDNA) substrates to dsDNA substrates and that it has higher elongation efficiency with 3′-OH than 3′-PO₄, which is conducive to detecting ALP [28]. In our method, 3′-OH-ended DNA, which is formed after ALP cleavage, generates the desired signal. TdT has little activity toward 3′-PO₄-ended DNA to generate the background signal (noise). A more significant signal-to-noise ratio (S/N) would result in a better LOD.

First, we optimized the structure of the substrate DNA strand, which had not been considered in previous studies [23–27]. We systematically studied the effect of substrates with different 3′-end structures on the elongation efficiency of TdT. As shown in Fig. 2A, we designed several structures such as ssDNA, hairpin dsDNA with a blunt end, and hairpin dsDNA with a sticky end. The 3′-end recessed with n bases is marked as 3′-n. The 3′-end protruded with n bases is marked as 3′+n. Fig. 2B shows the signal differences of these structures in response to TdT/Endo IV-assisted exponential amplification (without ALP) with 3′-PO₄ (blue column) or 3′-OH (orange column), respectively. The orange column reflects the potential largest signal after ALP cleavage, and the orange column indicates the noise when ALP is absent. A larger S/N (3′-OH/3′-PO₄, black line in Fig. 2B) indicates a potentially better ALP detection sensitivity. For the commonly used ssDNA substrate for TdT elongation, the S/N ratio was 9.8. When dealing with dsDNA substrates
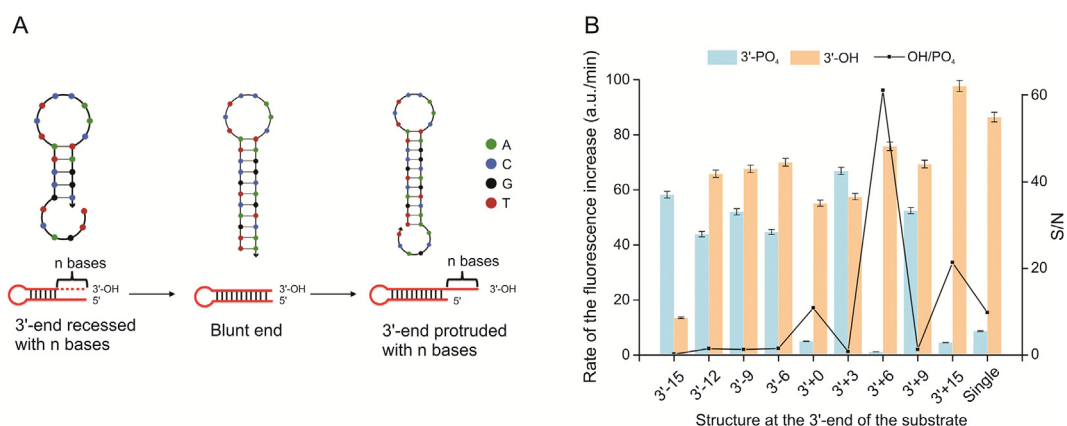
Fig. 2. (A) A schematic depiction of the dsDNA structures with different 3'-end. (B) The rate of fluorescence increase for different dsDNA with 3'-OH (the signal, orange column) and 3'-PO$_4$ (the noise, blue column). The signal to noise ratio (S/N, black line) was calculated for each column.

with different structures, the S/N for most of them became smaller. However, to our surprise, the 3'+6 dsDNA showed a dramatic S/N increase to be 61.1 as the noise of 3'+6 dsDNA (3'-PO$_4$ substrate) decreased compared to the noise of other substrates. We tested the noise of 3'+6 and 3'+9 dsDNA with different sequences to determine the cause. As shown in Fig. S3, the noise changed significantly, even with a single-base difference at the 3'-end. The data shown in Fig. 2B and Fig. S3 indicated that the length and sequence of the 3' protruded end in dsDNA affected the TdT elongation performance. The rules and mechanisms of this phenomenon are not clear and require further exploration. We selected 3'+6 dsDNA as a suitable substrate for ALP in the following experiments to obtain the best S/N in the substrates we tested.

We then optimized the substrate concentration (Fig. S4) and the enzyme concentration (Fig. S5) to achieve maximum detection. The optimized conditions for conducting further experiments were 100 nM substrate, 4 U/mL Endo IV, 100 U/mL TdT, 30 min for ALP dephosphorylation, and 30 min for TdT elongation.

3.3. Sensitivity of the method

With the best experimental conditions, we tested the signal of the system with varying concentrations of ALP. As shown in Fig. 3A, when the ALP concentration was increased, the fluorescence intensity also increased in exponential amplification curves. To determine the relationship between fluorescence intensity and ALP concentration, we chose the point of inflection (POI) values in each fluorescence curve for the quantitative detection of ALP in this assay. POI is defined as the number of fluorescence acquisition cycles (the fluorescence intensity was recorded at 20 s per cycle in the experiment) corresponding to the maximum slope in the sigmoidal curve. POI has been widely adopted in the EXPAR method for quantification [29]. According to the linear regression (Fig. 3B), POI and ALP concentration showed linear relation in the range of 0–0.4 U/L, and the LOD was 4.3×10^{-3} U/L. The LOD is better than that in most previous reports (Table S2) [26,27,30–53]. Our total detection time is approximately 80 min, which is acceptable for biological applications because of its high sensitivity. We also tested the stability and reproducibility of the proposed method. As shown in Table S3, the intraday relative standard deviations (RSD) were 1.6%–3.5%, and the interday RSD was 4.3% when measuring 0.1 U/L ALP.

3.4. Selectivity of the method

To evaluate the selectivity of our detection system for ALP, we selected the widely existing nucleases (Exo III, T7 exo, and DNase I),
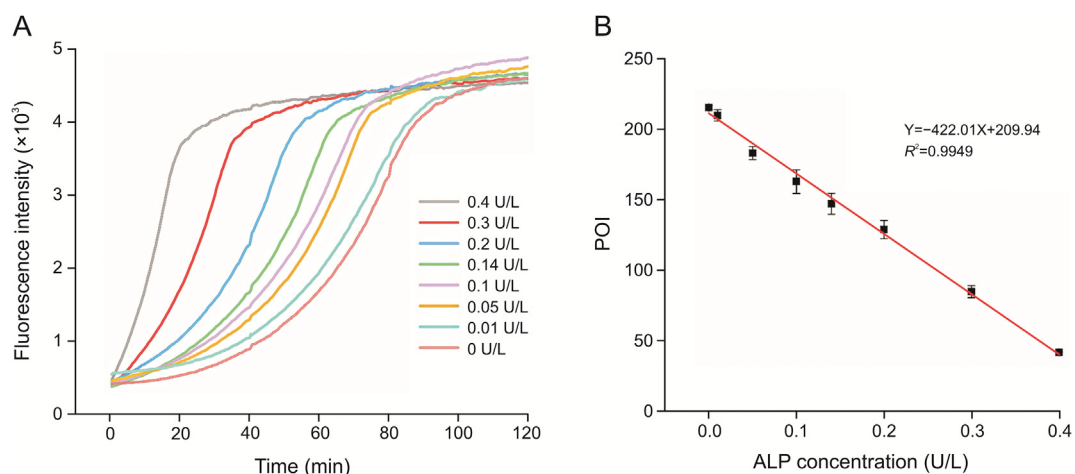

Fig. 3. (A) Fluorescence responses of TdT/Endo IV-assisted amplification with different ALP concentrations from 0 to 0.4 U/L. (B) The linear regression of the POI with ALP ranging from 0 to 0.4 U/L (0, 0.01, 0.05, 0.1, 0.14, 0.2, 0.3, and 0.4). The LOD can be calculated to be 4.3×10^{-3} U/L by 3σ/K. TdT: terminal deoxynucleotidyl transferase; Endo IV: endonuclease IV; ALP: alkaline phosphatase; POI: point of inflection; LOD: limit of detection.
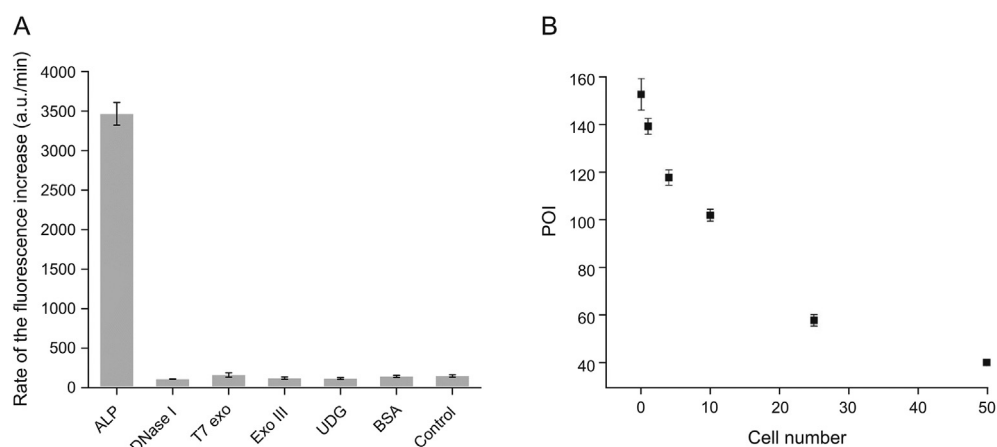
Fig. 4. (A) Selectivity evaluation for the proposed methods. The ALP concentration was 1 U/L. The concentrations of DNase I, T7 exo, Exo III, UDG were 10 U/L. The concentration of BSA was 0.1 mg/mL. Control means that there were no tested proteins. (B) The POI of the fluorescence response curves of the ALP detection system to the HeLa cell lysate diluted with different cell numbers from 0 to 50 (0, 1, 4, 10, 25, and 50). There was a statistical difference among the data sets in the groups for cell numbers with 0 and 1 ($t = 2.599$, $P < 0.05$). ALP: alkaline phosphatase; DNase I: deoxyribonuclease I; T7 exo: T7 exonucleas; Exo III: exonuclease III; UDG: uracil glycosylase; BSA: bovine serum albumin; POI: point of inflection.

enzyme (UDG), and protein (BSA). As shown in Fig. 4A, all the interfering proteins, whose concentrations were ten times that of ALP, produced a small fluorescence signal slightly as compared to the control (without testing proteins). Thus, our system could detect ALP with high specificity. Next, we measured ALP activity in HeLa cell lysates. As shown in Fig. 4B, our method could detect ALP activity in as low as only one cell.

4. Conclusion

In summary, we constructed a novel ALP amplification detection system based on TdT and Endo IV. A good S/N ratio was obtained by optimizing the DNA substrate structure, and exponential amplification was achieved using TdT and Endo IV. The advantages of the method for ALP detection can be summarized as follows: first, the LOD of our method shows that it is one of the most sensitive detection methods. Second, a good LOD was obtained without complicated reaction design or the synthesis of organic compounds or nanomaterials. Third, our method shows good selectivity for nucleases, which are critical interferents in practical application in clinical or biological samples such as serum and cell lysate. However, our method has some limitations. As two enzymes were used, the cost and operational complexity increased to a certain extent. Nevertheless, this work has the potential to improve disease diagnosis and wider biomedical applications, such as evaluation of ALP activity in human serum or cell lysate, screening of ALP inhibitors, quantitative labeling, and ELISAs.

CRediT author statement

Weicong Ye: Methodology, Investigation, Writing - Original draft preparation; **Longjie Li:** Methodology, Investigation, Writing - Reviewing and Editing; **Zishan Feng:** Investigation; **Bocheng Tu:** Investigation; **Zhe Hu:** Investigation; **Xianjin Xiao:** Resources; **Tongbo Wu:** Supervision, Conceptualization, Funding acquisition, Writing - Reviewing and Editing.

Declaration of competing interest

The authors declare that there are no conflicts of interest.

Appendix A. Supplementary data

Supplementary data to this article can be found online at https://doi.org/10.1016/j.jpha.2021.09.012.

References

[1] J.E. Coleman, Structure and mechanism of alkaline phosphatase, Annu. Rev. Biophys. Biomol. Struct. 21 (1992) 441–483.
[2] P. Colombatto, A. Randone, G. Civitico, et al., Hepatitis G virus RNA in the serum of patients with elevated gamma glutamyl transpeptidase and alkaline phosphatase: a specific liver disease, J. Viral Hepat. 3 (1996) 301–306.
[3] D.M. Goldberg, J.V. Martin, A.H. Knight, Elevation of serum alkaline phosphatase activity and related enzymes in diabetes mellitus, Clin. Biochem. 10 (1977) 8–11.
[4] Q.S. You, B.K.N. Choy, J.C.H. Chan, et al., Prevalence and causes of visual impairment and blindness among adult Chinese in Hong Kong—the Hong Kong eye study, Ophthalmic Epidemiol. 27 (2020) 354–363.
[5] S. Duhamel, S.T. Dyhrman, D.M. Karl, Alkaline phosphatase activity and regulation in the north pacific subtropical gyre, Limnol. Oceanogr. 55 (2010) 1414–1425.
[6] C. Labry, D. Delmas, A. Herbland, Phytoplankton and bacterial alkaline phosphatase activities in relation to phosphate and DOP availability within the Gironde plume waters (Bay of Biscay), J. Exp. Mar. Biol. Ecol. 318 (2005) 213–225.
[7] L. Jin, Y. Dong, X. Wu, et al., Versatile and amplified biosensing through enzymatic cascade reaction by coupling alkaline phosphatase in situ generation of photoresponsive nanozyme, Anal. Chem. 87 (2015) 10429–10436.
[8] H. Jang, J. Ahn, M. Kim, et al., Electrical signaling of enzyme-linked immunosorbent assays with an ion-sensitive field-effect transistor, Biosens. Bioelectron. 64 (2015) 318–323.
[9] Q. Huang, C. He, J. Zhang, et al., Unlocking the hidden talent of DNA: unexpected catalytic activity for colorimetric assay of alkaline phosphatase, Anal. Chim. Acta 1055 (2019) 98–105.
[10] J. Barroso, L. Saa, R. Grinyte, et al., Photoelectrochemical detection of enzymatically generated CdS nanoparticles: application to development of immunoassay, Biosens. Bioelectron. 77 (2016) 323–329.
[11] S. Goggins, C. Naz, B.J. Marsh, et al., Ratiometric electrochemical detection of alkaline phosphatase, Chem. Commun. 51 (2015) 561–564.
[12] C.M. Li, S.J. Zhen, J. Wang, et al., A gold nanoparticles-based colorimetric assay for alkaline phosphatase detection with tunable dynamic range, Biosens. Bioelectron. 43 (2013) 366–371.

[13] C. Ruan, W. Wang, B. Gu, Detection of alkaline phosphatase using surface-enhanced Raman spectroscopy, Anal. Chem. 78 (2006) 3379–3384.

[14] M. Lin, J. Huang, F. Zeng, et al., A fluorescent probe with aggregation-induced emission for detecting alkaline phosphatase and cell imaging, Chem. Asian J. 14 (2018) 802–808.

[15] J. Sun, J. Zhao, X. Bao, et al., Alkaline phosphatase assay based on the chromogenic interaction of diethanolamine with 4-aminophenol, Anal. Chem. 90 (2018) 6339–6345.

[16] Y. Tan, L. Zhang, K.H. Man, et al., Reaction-based off-on near-infrared fluorescent probe for imaging alkaline phosphatase activity in living cells and mice, ACS Appl. Mater. Interfaces 9 (2017) 6796–6803.

[17] H. Liu, Z. Lv, K. Ding, et al., Incorporation of tyrosine phosphate into tetraphenylethylene affords an amphiphilic molecule for alkaline phosphatase detection, hydrogelation and calcium mineralization, J. Mater. Chem. B. 1 (2013) 5550–5556.

[18] X. Niu, Y. He, X. Li, et al., A peroxidase-mimicking nanosensor with Hg^{2+}-triggered enzymatic activity of cysteine-decorated ferromagnetic particles for ultrasensitive Hg^{2+} detection in environmental and biological fluids, Sensor. Actuator. B Chem. 281 (2019) 445–452.

[19] X. Xu, X. Zou, S. Wu, et al., In situ formation of fluorescent polydopamine catalyzed by peroxidase-mimicking FeCo-LDH for pyrophosphate ion and pyrophosphatase activity detection, Anal. Chim. Acta 1053 (2019) 89–97.

[20] X. Niu, Y. He, J. Pan, et al., Uncapped nanobranch-based CuS clews used as an efficient peroxidase mimic enable the visual detection of hydrogen peroxide and glucose with fast response, Anal. Chim. Acta 947 (2016) 42–49.

[21] S. Liu, X. Wang, S. Pang, et al., Fluorescence detection of adenosine-5'-triphosphate and alkaline phosphatase based on the generation of CdS quantum dots, Anal. Chim. Acta 827 (2014) 103–110.

[22] W. Gorczyca, J. Gong, Z. Darzynkiewicz, Detection of DNA strand breaks in individual apoptotic cells by the in situ terminal deoxynucleotidyl transferase and nick translation assays, Can. Res. 53 (1993) 1945–1951.

[23] Y. Du, S. Wang, X. Li, et al., Terminal deoxynucleotidyl transferase-activated nicking enzyme amplification reaction for specific and sensitive detection of DNA methyltransferase and polynucleotide kinase, Biosens. Bioelectron. 145 (2019) 111700.

[24] Y. Du, Y. Cui, X. Li, et al., Terminal deoxynucleotidyl transferase and T7 exonuclease-aided amplification strategy for ultrasensitive detection of uracil-DNA glycosylase, Anal. Chem. 90 (2018) 8629–8634.

[25] K. Shi, B. Dou, J. Yang, et al., Target-triggered catalytic hairpin assembly and TdT-catalyzed DNA polymerization for amplified electronic detection of thrombin in human serums, Biosens. Bioelectron. 87 (2017) 495–500.

[26] Y. Liu, E. Xiong, X. Li, et al., Sensitive electrochemical assay of alkaline phosphatase activity based on TdT-mediated hemin/G-quadruplex DNAzyme nanowires for signal amplification, Biosens. Bioelectron. 87 (2017) 970–975.

[27] Y. Wang, L. Yang, N. Li, et al., A versatile assay for alkaline phosphatase detection based on thymine-Hg(II)-thymine structure generation mediated by TdT, Talanta 195 (2019) 566–572.

[28] I. Sarac, M. Hollenstein, Terminal deoxynucleotidyl transferase in the synthesis and modification of nucleic acids, Chembiochem 20 (2019) 860–871.

[29] M.S. Reid, X.C. Le, H. Zhang, Exponential isothermal amplification of nucleic acids and assays for proteins, cells, small molecules, and enzyme activities: an EXPAR example, Angew. Chem., Int. Ed. Engl. 57 (2018) 11856–11866.

[30] H. Wang, C. Ma, Z. Li, et al., An exonuclease-assisted fluorescence sensor for assaying alkaline phosphatase based on SYBR Green I, Mol. Cell. Probes 45 (2019) 26–30.

[31] Y. Zhang, Y. Wang, S.F.A. Rizvi, et al., Detection of DNA 3'-phosphatase activity based on exonuclease III-assisted cascade recycling amplification reaction, Talanta 204 (2019) 499–506.

[32] H. Liu, C. Ma, J. Wang, et al., A turn-on fluorescent method for determination of the activity of alkaline phosphatase based on dsDNA-templated copper nanoparticles and exonuclease based amplification, Microchim. Acta. 184 (2017) 2483–2488.

[33] J. Zhang, W. Zhao, W. Zhang, et al., A path-choice-based biosensor to detect the activity of the alkaline phosphatase as the switch, Anal. Chim. Acta 1135 (2020) 64–72.

[34] X. Liu, Z. Cheng, S. Zhang, et al., Amplification strategy of silver nanoclusters with a satellite-nanostructure for substrate-free assay of alkaline phosphatase by ICP-ms, Anal. Chem. 92 (2020) 3769–3774.

[35] X. Liu, X. Li, X. Gao, et al., A universal paper-based electrochemical sensor for zero-background assay of diverse biomarkers, Acs Appl. Mater. Inter. 11 (2019) 15381–15388.

[36] L. Wang, Z. Wang, C. Zhang, Primer dephosphorylation-initiated circular exponential amplification for ultrasensitive detection of alkaline phosphatase, Analyst 143 (2018) 4606–4613.

[37] Z. Qian, L. Chai, C. Tang, et al., Carbon quantum dots-based recyclable real-time fluorescence assay for alkaline phosphatase with adenosine triphosphate as substrate, Anal. Chem. 87 (2015) 2966–2973.

[38] H. Huang, B. Wang, M. Chen, et al., Fluorescence turn-on sensing of ascorbic acid and alkaline phosphatase activity based on graphene quantum dots, Sensor. Actuator. B Chem. 235 (2016) 356–361.

[39] J. Liu, D. Tang, Z. Chen, et al., Chemical redox modulated fluorescence of nitrogen-doped graphene quantum dots for probing the activity of alkaline phosphatase, Biosens. Bioelectron. 94 (2017) 271–277.

[40] Y. Chen, W. Li, Y. Wang, et al., Cysteine-directed fluorescent gold nanoclusters for the sensing of pyrophosphate and alkaline phosphatase, J. Mater. Chem. C. 2 (2014) 4080–4085.

[41] H. Liu, M. Li, Y. Xia, et al., A turn-on fluorescent sensor for selective and sensitive detection of alkaline phosphatase activity with gold nanoclusters based on inner filter effect, ACS Appl. Mater. Interfaces 9 (2017) 120–126.

[42] X.L. Hu, X.M. Wu, X. Fang, et al., Switchable fluorescence of gold nanoclusters for probing the activity of alkaline phosphatase and its application in immunoassay, Biosens. Bioelectron. 77 (2016) 666–672.

[43] X. Ren, Z. Chen, X. Chen, et al., Sensitive optical detection of alkaline phosphatase activity with quantum dots, J. Lumin. 145 (2014) 330–334.

[44] G. Mao, Q. Zhang, Y. Yang, et al., Facile synthesis of stable CdTe/CdS QDs using dithiol as surface ligand for alkaline phosphatase detection based on inner filter effect, Anal. Chim. Acta 1047 (2019) 208–213.

[45] S. Liu, S. Pang, W. Na, et al., Near-infrared fluorescence probe for the determination of alkaline phosphatase, Biosens. Bioelectron. 55 (2014) 249–254.

[46] X. You, C. Huang, Y. Luo, et al., A smartphone-based platform for point-of-use determination of alkaline phosphatase as an indicator of water eutrophication, Microchim. Acta. 187 (2020), 354.

[47] H. Li, Q. Yao, F. Xu, et al., An activatable AIEgen probe for high-fidelity monitoring of overexpressed tumor enzyme activity and its application to surgical tumor excision, Angew. Chem., Int. Ed. Engl. 59 (2020) 10186–10195.

[48] C. Chen, J. Zhao, Y. Lu, et al., Fluorescence immunoassay based on the phosphate-triggered fluorescence turn-on detection of alkaline phosphatase, Anal. Chem. 90 (2018) 3505–3511.

[49] C. Ma, H. Tan, L. Chen, et al., A terbium chelate based fluorescent assay for alkaline phosphatase in biological fluid, Sensor. Actuator. B Chem. 202 (2014) 683–689.

[50] R. Kong, T. Fu, N. Sun, et al., Pyrophosphate-regulated Zn^{2+}-dependent DNAzyme activity: an amplified fluorescence sensing strategy for alkaline phosphatase, Biosens. Bioelectron. 50 (2013) 351–355.

[51] H. Zhang, C. Xu, J. Liu, et al., An enzyme-activatable probe with a self-immolative linker for rapid and sensitive alkaline phosphatase detection and cell imaging through a cascade reaction, Chem. Commun. 51 (2015) 7031–7034.

[52] C.Y. Lee, K.S. Park, H.G. Park, A simple, sensitive, and label-free assay for alkaline phosphatase activity based on target-promoted exponential strand displacement amplification, Sensor. Actuator. B Chem. 262 (2018) 1001–1005.

[53] J. Liang, R.T.K. Kwok, H. Shi, et al., Fluorescent light-up probe with aggregation-induced emission characteristics for alkaline phosphatase sensing and activity study, Acs Appl. Mater. Inter. 5 (2013) 8784–8789.